Monthly Notices
of the
ROYAL ASTRONOMICAL SOCIETY

MNRAS **481,** 3313–3324 (2018)
Advance Access publication 2018 September 10

doi:10.1093/mnras/sty2461

Hubble Space Telescope FUV observations of M31's globular clusters suggest a spatially homogeneous helium-enriched subpopulation

Mark B. Peacock [1]★ Stephen E. Zepf,[1] Thomas J. Maccarone,[2] Arunav Kundu,[3] Christian Knigge,[4] Andrea Dieball[5] and Jay Strader[1]

[1] *Michigan State University, East Lansing, MI 48824, USA*
[2] *Texas Tech University, Lubbock, TX 79409, USA*
[3] *Eureka Scientific Inc., 2452 Delmer Street, Suite 100 Oakland, CA 94602, USA*
[4] *University of Southampton, Southampton SO17 1BJ, UK*
[5] *Universität Bonn, Auf dem Hügel 71, D-53121 Bonn, Germany*

Accepted 2018 September 5. Received 2018 September 5; in original form 2018 June 14

ABSTRACT

We present high spatial resolution, far ultraviolet (FUV) F140LP observations of 12 massive globular clusters in M 31 obtained using the ACS/SBC on the Hubble Space Telescope (*HST*). These observations resolve the cluster profiles to scales similar to their core radii and enable the study of the spatial distribution of blue and extreme horizontal branch (HB) stars, which dominate the emission in the F140LP images. We confirm that some of these clusters have excess FUV emission, suggesting additional hot populations beyond those expected by canonical single stellar population models. We find no evidence that the hot populations are spatially distinct from the majority populations in these clusters, as would be expected if the excess FUV emission is a result of a dynamically enhanced population of extreme-HB stars. We conclude that a second population of stars with significantly enhanced helium abundance is a viable explanation for the observed FUV emission that is both bright and distributed similarly to the rest of the cluster light. Our results support the use of FUV observations as a path to characterizing helium-enhanced subpopulations in extragalactic clusters. These M 31 clusters also show a correlation such that more massive and denser clusters are relatively FUV bright. Similar to extant Milky Way results, this may indicate the degree of helium enrichment, or second population fraction increases with cluster mass.

Key words: stars: horizontal branch – globular clusters: general – galaxies: individual: M 31 – galaxies: star clusters: general – ultraviolet: galaxies.

1 INTRODUCTION

Far ultraviolet (FUV) observations are a unique probe of hot stellar populations. In old systems, such as globular clusters and early-type galaxies, their main sequence and red giant branch stars are generally too cool to emit significantly at such wavelengths. Instead, their FUV emission is dominated by their much rarer hot populations.

A surprising result from early observations of passive, red early-type galaxies is that they are brighter in the FUV than expected; exhibiting a 'UV-upturn' (e.g. Code 1969; Dorman, O'Connell & Rood 1995; O'Connell 1999). Recent studies, based on *Galaxy Evolution Explorer* (*GALEX*) observations, have noted that only a fraction of early-type galaxies exhibit a true UV upturn, defined as increasing F_λ with λ below $\sim$2000 Å (Yi et al. 2011). However, the vast majority still exhibit significant excess FUV emission compared to that expected based on their spectral energy distributions from the near-UV through infrared (Smith, Lucey & Carter 2012). The leading explanation for this excess FUV emission from old populations is the presence of extreme horizontal branch (HB) stars (Greggio & Renzini 1990; O'Connell 1999; Brown et al. 2000). This hypothesis is supported by *HST* observations of M32, which favour a blue-/extreme-HB star explanation for its UV upturn (Brown et al. 2008). While HB stars are an expected phase of stellar evolution, the magnitude of the FUV excess and the origin of the hottest extreme-HB stars in metal-rich environments is quite poorly understood. Several mechanisms have been proposed to produce these stars, including high mass-loss on the red giant branch at high metallicity (Greggio & Renzini 1990); binary interactions (Han, Podsiadlowski & Lynas-Gray 2007); and helium-enhanced subpopulations (Lee et al. 2005; Chung, Yoon & Lee 2011).

Globular clusters are prime environments to study HB stars due to their similar ages and metallicities. Dynamical interactions between stars also effect the binary populations in the clusters, allowing us to

★ E-mail: mpeacock@msu.edu

© 2018 The Author(s)
Published by Oxford University Press on behalf of the Royal Astronomical Society

Downloaded from https://academic.oup.com/mnras/article-abstract/481/3/3313/5094594 by University of Southampton user on 07 November 2018

study the influence of such interactions on the evolution of HB stars. Studies of the Galactic globular clusters have shown that they host complex-HB star morphologies. The HB stars in lower metallicity clusters are, on average, bluer than those in metal-rich clusters and metallicity has long been proposed as the 'first parameter' effecting the HB stars (Sandage & Wallerstein 1960). However, metallicity alone cannot explain the observations. For example, different HB star populations are observed in similar metallicity clusters (e.g. Bellazzini et al. 2001). Metallicity also appears to have less of an influence on the 'tail' of the HB star morphology (i.e. the presence of very hot, extreme-HB stars, e.g. O'Connell 1999) than it does on the fraction of stars redder or bluer than the instability strip. These complexities of the HB phase of stellar evolution led to the infamous 'second parameter' problem and several additional parameters have been proposed to influence these stars such as age, helium abundance (and second population stars), stellar core rotation, and the stellar density in the cluster core (for a discussion, see e.g. Catelan 2009).

In recent years, increased helium abundance has been proposed as a natural explanation for the formation of bluer HB stars. This is due to the compelling evidence that most of the Galactic globular clusters are not true simple stellar populations, but rather host at least two populations, with the 'second population' having significantly different abundances of light and intermediate-mass elements (see e.g. the reviews of Gratton, Carretta & Bragaglia 2012; Bastian & Lardo 2018; and references therein). Current theories for the formation of these multiple populations struggle to explain all of the observations (e.g. Bastian 2015). However, most require that the second population stars are significantly enriched in helium (e.g. D'Antona & Ventura 2007; Bragaglia et al. 2010). Such enhanced helium fractions have been observed in spectroscopic observations of a small number of cluster stars (e.g. Marino et al. 2011, 2014; Pasquini et al. 2011) and can explain the observed *HST* colour–magnitude diagrams of many clusters (e.g. Milone et al. 2012; Piotto et al. 2013; Milone 2015). Based on current samples, the fraction of second populations stars and their helium enrichment appears to vary significantly in different clusters (with $0.01 < \Delta Y < 0.12$) and may correlate with cluster mass (Wagner-Kaiser et al. 2016; Milone et al. 2017). The combination of first population stars and helium-enhanced second population stars can help to explain the complex HB star morphologies observed in the Galactic globular clusters (e.g. D'Antona et al. 2005; Joo & Lee 2013; Lee et al. 2005).

Another potentially important mechanism for the formation of extreme-HB stars in the dense cores of globular clusters is dynamical formation. Several dynamical processes may produce these very hot HB stars. First, close encounters may produce bluer HB stars both through enhanced mass-loss from tidal stripping and via helium dredge up into the stellar atmosphere (e.g. Suda et al. 2007; Pasquato et al. 2014). It is also thought that mass-loss in binary interactions is an important mechanism for forming extreme-HB stars in the Galactic field (aka subdwarf B stars; Maxted et al. 2001; Han et al. 2003). The dense stellar environments in the cores of globular clusters are known to significantly influence binary properties (e.g. Heggie 1975) and may therefore influence the formation of extreme-HB stars. Additionally, the tightening of binaries via stellar interactions may cause a binary of two helium white dwarfs to merge – producing an extreme-HB like star (Han et al. 2003; Han 2008). If any of these processes are important in the production of extreme-HB stars, then the formation of these stars should be enhanced in the cores of clusters with higher stellar densities. Studies of the Galactic globular clusters have tried to test for this correlation, but claims there is a correlation (Fusi Pecci et al. 1993; Buonanno et al. 1997; Rich et al. 1997; Dotter et al. 2010) have been intermixed with those that suggest there may not be (e.g. van den Bergh & Morris 1993; Recio-Blanco et al. 2006; Dalessandro et al. 2012).

Recent modelling of HB stars has suggested that both of these effects – enhanced mass-loss due to dynamical interactions and helium enhancement – may be required to produce the hottest extreme-HB stars (Yaron et al. 2017).

Extending the study of HB stars to globular clusters beyond the Milky Way and its satellites enables us to improve our understanding of them by expanding the sample – especially important for those that are rare in the Milky Way, such as massive and metal-rich clusters. To this end, we present in this paper new, high spatial resolution FUV observations of M 31's globular clusters. At these wavelengths, a population of blue-/extreme-HB stars will dominate the emission from globular clusters (e.g. Moehler 2001) – this is because other hot populations are either orders of magnitude fainter than these stars (such as white dwarfs and cataclysmic variables) or they are too rare to dominate over such a population (such as post-AGB stars and low-mass X-ray binaries). Observations of the Galactic globular clusters confirm that their integrated FUV colours correlate with their HB star morphology (Catelan 2009; Dalessandro et al. 2012).

In this paper, we consider a sample of 12 massive and FUV bright globular clusters in M 31 (see Section 2 for details), for which we present new high-resolution *HST* ACS/SBC F140LP observations (Section 3). We derive total FUV magnitudes of these clusters and compare to published photometry based on lower signal-to-noise ratio and lower spatial resolution *GALEX* observations (Section 3.2). We also present the ultraviolet surface brightness profiles at both F140LP (FUV) and F336W (u-band) wavelengths (Section 3.3), which we use to consider the distribution of hot HB stars in these clusters. We conclude by discussing the constraints that these data place on dynamically enhanced extreme-HB star populations (Section 4) and the evidence for second populations of helium-enhanced stars in these clusters (Section 5).

2 M 31'S GLOBULAR CLUSTERS

M 31 hosts the largest population of globular clusters in the Local Group (>400, e.g. Peacock et al. 2010a). At a distance of 744 kpc (Vilardell et al. 2010), this cluster system is an important bridge between the well studied and spatially resolved stellar populations in the Galactic globular clusters and the unresolved, but far more numerous, extra-galactic globular cluster systems.

Globular clusters at the distance of M 31 have median core radii, $r_c \sim 0.25$ arcsec (0.8 pc) and half-light radii, $r_h \sim 0.7$ arcsec (2.7 pc; Barmby et al. 2007; Peacock et al. 2010a). Observations using the *HST* therefore resolve their integrated emission to scales similar to their core radii, while brighter stars outside of the cluster cores can also be resolved in such observations (e.g. Brown et al. 2004; Perina et al. 2012).

This paper considers 12 of M 31's globular clusters. All of these clusters have published integrated photometry in the Sloan Digital Sky Survey (SDSS) *ugriz* bands (Peacock et al. 2010a) and *GALEX* FUV+NUV bands (Rey et al. 2007). These clusters are all quite bright and massive with $i < 14.8$ mag, which corresponds to mass, $M > 0.8 \times 10^6\,\mathrm{M}_\odot$ (assuming $i_\odot = 4.58$ mag and $M/L_i = 1.8$, based on a 12 Gyr simple stellar population with $[Z/H] = -1.35$ and a Kroupa IMF; Maraston 2005). The clusters are also known to be bright in the FUV ($FUV < 22.1$ mag; Rey et al. 2009). Additionally,

Downloaded from https://academic.oup.com/mnras/article-abstract/481/3/3313/5094594 by University of Southampton user on 07 November 2018

all of the clusters have relatively low extinction, with $E(B-V) < 0.16$ (Fan et al. 2008). This minimizes errors due to uncertainty in the extinction curve in the ultraviolet, which we take to have $R_{\rm FUV} = 8.2$ in the FUV (based on Cardelli, Clayton & Mathis 1989 and as used by Rey et al. 2007).

Structural parameters have been published for most of these clusters from ground-based *K*-band observations (Peacock et al. 2010a) and *HST* ACS or WFPC2 observations (Barmby et al. 2007; Strader, Caldwell & Seth 2011). For the remaining two clusters, we fit their F336W images using the ISHAPE code (Larsen 1999). For each cluster, we calculate the half-light relaxation time via (Binney & Tremaine 1987; McLaughlin & van der Marel 2005):

$$\tau_h = 2.06 \times \frac{10^6}{\ln(0.4 M_{\rm tot}/m_\star)} \frac{M_{\rm tot}^{0.5}}{m_\star} r_h^{1.5}, \quad (1)$$

where $m_\star$ is the average stellar mass. For all clusters, we take $m_\star = 0.5\,{\rm M}_\odot$. Table 1 lists our sample of globular clusters, their structural parameters, and integrated photometry. The final column shows the total FUV magnitudes derived from this study (see Section 3.2).

3 DATA AND ANALYSIS

3.1 High spatial resolution *HST* observations

To investigate the hot populations in these globular clusters, we obtained *HST* ACS/SBC observations through the F140LP filter under programme ID 14132 (PI: Peacock). These observations were taken in September and October of 2016 with each cluster observed for one orbit using a four point dither pattern, resulting in total exposure times for each cluster of 2713s. The F140LP filter has a pivot wavelength of 1528 Å and a similar transmission profile to the *GALEX* FUV filter. We utilize the pipeline reduced products for each exposure, the 'flt' files. For each cluster, we combine the four exposures together using the DRIZZLEPAC task ASTRODRIZZLE, run under ASTROCONDA. We drizzle combine on to a 0.025 arcsec grid with '$final\_pixfrac' = 1.0$.

Multi-wavelength *HST* observations of these clusters are also available at redder wavelengths from the Panchromatic Hubble Andromeda Treasury (PHAT) survey (Dalcanton et al. 2012). This provides near-UV WFC3/UVIS F275W + F336W observations and optical ACS/WFC F475W + F814W observations. We utilize the reduced and mosaicked WFC3/UVIS F336W 'brick' images provided by this survey.[1] These images have a pixel scale of 0.04 arcsec. For details of the reduction of these PHAT data, see Williams et al. (2014). For each cluster, we cut sections from these bricks that cover the ACS/SBC fields and align them using the DRIZZLEPAC task TWEAKREG.

Thumbnails of these ACS/SBC/F140LP (FUV) and WFC3/UVIS/F336W (similar to a *u*-band filter) images are presented in Fig. 1. We also show the clusters from *GALEX* FUV observations, which have a similar wavelength coverage to the F140LP filter, but a much lower spatial resolution. It can be seen that all of the clusters are well resolved in these *HST* images, with many of their brighter stars also resolved.

3.2 Integrated FUV photometry

We perform photometry on these images using the DAOPHOT/PHOT task, implemented under PYRAF. The flux is measure through a range of log-spaced apertures with radii, $0.05 < r < 5.0$ arcsec, which corresponds to $0.2 < r < 18.0$ pc at a distance of 744 kpc. The cluster centres were defined based on the F336W images of the clusters. Due to the higher stochasticity in the F140LP profiles, we fixed the cluster centres based on their locations in the aligned F336W images. We note that consistent profiles were also obtained using the STSDAS task ELLIPSE, but this task assumes a smooth positive gradient towards the cluster centre and failed to fit isophotes to the inner regions for some of the clusters, we therefore chose to use the simple aperture photometry instead.

We consider several different techniques and spatial regions for estimating the background level. The background in the F140LP images is found to be dominated by discrete point sources. We therefore choose to estimate the background level for all apertures as the mean value within a fixed sky annulus of 5–7 arcsec, with no sigma clipping.

The instrumental magnitudes are placed on the ABMAG system, using zero-points calculated from the calibrations provided by the *HST*/ACS pipeline using the relation:

$$m_{0,AB} = -2.5\log_{10}(PHOTFLAM) - 21.10 - 5.0\log_{10}(PHOTPLAM) + 18.6921. \quad (2)$$

For these F140LP data, $PHOTFLAM = 2.7128664 \times 10^{-17}$ and $PHOTPLAM = 1528.0$.

In addition to total magnitudes within each aperture, we also calculate the average surface brightness within each annulus as the difference in flux between successive apertures:

$$\mu_i = m_{0,AB} - 2.5\log_{10}\left(\frac{F_i - F_{i-1}}{A_i}\right). \quad (3)$$

Here, μ_i is the surface brightness in annulus i (in mag asec^{-2}), F_i is the flux within aperture i, and A_i is the area of the annulus (in asec^2).

In Fig. 2, we show the FUV magnitude of these clusters within a 5 arcsec aperture. This aperture corresponds to a physical scale of 18 pc and, while cluster stars may be expected beyond this radius, the surface brightness profiles are found to be consistent with the sky level at this distance. We compare these magnitudes to *GALEX* photometry of the clusters, as published by Rey et al. (2007). Because of the large *GALEX* PSF, these clusters are consistent with point sources in such observations and their photometry was obtained through a 4.5 arcsec aperture with an aperture correction derived from bright stars in the image.

For 11 of the 12 clusters observed our *HST*/SBC/F140LP photometry is consistent with a slight offset from the *GALEX* FUV photometry, with $F140LP = FUV - 0.27$. Some of this offset may result from either differences in the estimation of the background level or from the aperture correction applied to the *GALEX* observations. However, the clusters may also be slightly brighter in these F140LP observations due to a red leak (which is known to affect ACS/SBC observations; Boffi et al. 2008). In Peacock et al. (2017), a small red-leak was also suggested in FUV photometry of M87's globular clusters, based on comparing observations obtained using the similarly designed *HST* STIS MAMA detector with the alternate technology and independently calibrated WFPC2 detector. We therefore caution that ∼20 per cent of the FUV flux in these F140LP observations may come from redder wavelengths. We propose that such a correction should be considered when analysing *HST* ACS/SBC or STIS FUV observations of globular clusters. Ideally, the now recommended 'dual filter' approach can be used to

[1] Obtained from https://archive.stsci.edu/prepds/phat/datalist.html.

Downloaded from https://academic.oup.com/mnras/article-abstract/481/3/3313/5094594 by University of Southampton user on 07 November 2018

Table 1. M 31 globular cluster properties and FUV photometry.

Name[a]	g^a	$g-i^a$	M^b (10^6 $M_\odot$)	[Fe/H][c]	$E(B-V)^c$	r_h [d] (pc)	τ_h [d] (Gyr)	μ_0 [d] (mag asec^{-2})	*GALEX* [e] FUV	*GALEX* [e] NUV	*HST* [f] *F*140*LP*
B127-G185	14.16	1.21	4.3	−0.80	0.09	2.56	2.3	17.32	20.66 ± 0.11	19.39 ± 0.08	20.36 ± 0.02
B131-G189	15.33	0.83	1.0	−0.81	0.12	1.83	0.8	16.55	20.81 ± 0.13	19.89 ± 0.11	20.52 ± 0.03
B178-G229	14.91	0.73	1.4	−1.51	0.12	2.20	1.1	17.49	19.48 ± 0.03	18.73 ± 0.02	19.27 ± 0.01
B179-G230	15.36	0.83	1.0	−1.10	0.10	2.69	1.3	17.38	21.67 ± 0.14	19.91 ± 0.04	21.68 ± 0.03
B193-G244	15.36	1.09	1.3	−0.44	0.11	2.03	1.0	16.93	21.96 ± 0.10	21.24 ± 0.05	23.12 ± 0.20
B205-G256	15.29	0.78	1.0	−1.34	0.14	2.16	1.0	17.95	22.07 ± 0.19	20.10 ± 0.03	21.70 ± 0.03
B206-G257	14.94	0.75	1.4	−1.45	0.13	2.81	1.6	17.70	20.43 ± 0.04	19.20 ± 0.02	20.09 ± 0.01
B218-G272	14.55	0.83	2.1	−1.19	0.14	3.19	2.4	16.33	19.74 ± 0.05	19.07 ± 0.02	19.41 ± 0.01
B224-G279	15.10	0.66	1.1	−1.80	0.13	6.95	5.8	20.26	20.78 ± 0.05	19.36 ± 0.02	20.46 ± 0.01
B225-G280	14.21	0.99	3.4	−0.67	0.10	2.12	1.6	15.71	20.17 ± 0.05	19.33 ± 0.02	19.84 ± 0.01
B232-G286	15.46	0.67	0.8	−1.83	0.14	2.43	1.0	17.25	20.67 ± 0.06	19.49 ± 0.02	20.34 ± 0.01
B472-D064	15.06	0.75	1.2	−1.45	0.13	1.71	0.7	17.03	19.94 ± 0.04	19.03 ± 0.02	19.84 ± 0.03

[a]Dereddened 'total' g-band magnitude and $g-i$ colour from Sloan Digital Sky Survey photometry (Peacock et al. 2010a).
[b]Mass of the cluster inferred from i-band mag, assuming a distance modulus of 24.36 and a mass-to-light ratio $M/L_i = 1.8$ (Maraston 2005).
[c]Metallicity and extinction (Fan et al. 2008, and references therein). Higher resolution spectroscopy is only available for a few of these clusters, but we note that the authors caution significant systematic errors may exist in these low-resolution metallicities (Colucci et al. 2009; Sakari et al. 2016). Throughout this paper, we utilize optical colour as a proxy for metallicity.
[d]The half-light radius (r_h), half-light relaxation time (τ_h, from equation 1), and central F336W surface brightness (μ_0, see Section 3.3).
[e]'Total' FUV and NUV magnitudes from *GALEX* photometry (Rey et al. 2007).
[f]'Total' FUV magnitudes (within a 5 arcsec aperture) from our F140LP observations (see Section 3.2).

directly identify and remove such red leak (such as the recent observations of clusters in NGC 3115; Proposal ID 14738, PI: Kundu).

These F140LP observations do confirm significant FUV emission from these clusters. Additionally, we find no evidence for a trend with luminosity when comparing to the *GALEX* observations, as might be expected if contamination was effecting the *GALEX* observations. We therefore confirm that the published *GALEX* integrated photometry of these clusters is likely reliable, despite the low spatial resolution and signal-to-noise ratio of the observations. This includes two metal-rich clusters (B127 and B225) that are much more luminous in the FUV than predicted by canonical models for HB star morphology (see Rey et al. 2007; Peacock et al. 2017; and Section 5).

One cluster (B193) is found to be significantly fainter in our observations. As can be seen in Fig. 1, this cluster is extremely faint in these F140LP observations. We note that this source is a low significance detection in the *GALEX* photometry and believe its published photometry may be unreliable due to either contamination from nearby sources or errors in the background estimation.

3.3 Radial profiles in the ultraviolet: *FUV*- and *u*-bands

Fig. 3 shows the surface brightness profiles of our sample of 12 clusters in F140LP (FUV, blue points) and F336W (u, red points). For comparison with the cluster profiles, the dashed-grey lines in Fig. 3 show the profile expected for a point source. This is estimated using the TinyTim simulations (Krist, Hook & Stoehr 2011).[2] Profiles are constructed from the resulting PSF images in a similar fashion to the cluster images and scaled to match the cluster surface brightness at 0.05 arcsec. It can be seen that all of the clusters are well resolved.

The F140LP profiles reflect some stochasticity from the fact that the light is dominated by less numerous blue and extreme-HB stars, while redder bands, including F336W, are dominated by much more numerous, cooler stars. Detailed comparison confirms that the ripples in the profiles are produced by individual FUV bright stars. We choose not to subtract these stars from the profiles since cluster stars could be this bright and the magnitude to which we remove FUV bright stars would be arbitrary.

With the exception of features associated with individual FUV bright point sources, the profiles of the clusters are found to be quite similar at F140LP and F336W wavelengths. To better consider variations in the profiles, we show in Fig. 4 the $F140LP - F336W$ profiles of the clusters. These figures include the weighted mean colour of clusters over the full radial region considered ($r < 5$ arcsec; solid black line). The average $FUV - u$ colours of the clusters are found to vary by 2.5 mag. Some variation is observed in the colour with radius. This can generally be attributed to individual bright sources. However, no significant trends in the colours of these clusters with radius are observed.

3.4 Distribution of blue-/extreme-HB stars

The $F140LP - F336W$ colour probes the HB star morphology. This is because the presence of very hot blue-/extreme-HB stars will strongly influence the FUV flux, but will have far less effect on redder bands (including F336W) that will be dominated by emission from more common cooler stars. Therefore, these surface brightness profiles in F140LP and F336W can be used to test whether the hot populations in these clusters are spatially distinct. We identify no significant radial trends in the $F140LP - F336W$ colours of these clusters. These data therefore suggest that the blue-/extreme-HB stars are well mixed with the other stellar populations.

Similar FUV profiles have not been published for the Galactic globular clusters. However, the distribution of the resolved HB populations have been studied in some of these clusters (e.g. Iannicola et al. 2009; Vanderbeke et al. 2015). Vanderbeke et al. (2015) recently traced the radial distribution of red, blue, and extreme-HB stars in 48 Galactic globular clusters, by identifying the populations in ground based optical g- and z-band photometry. This work is sensitive to a similar radial range to our surface brightness profiles, from around the core/half-light radius to a few half-light radii.

[2]http://tinytim.stsci.edu/cgi-bin/tinytimweb.cgi

Downloaded from https://academic.oup.com/mnras/article-abstract/481/3/3313/5094594 by University of Southampton user on 07 November 2018

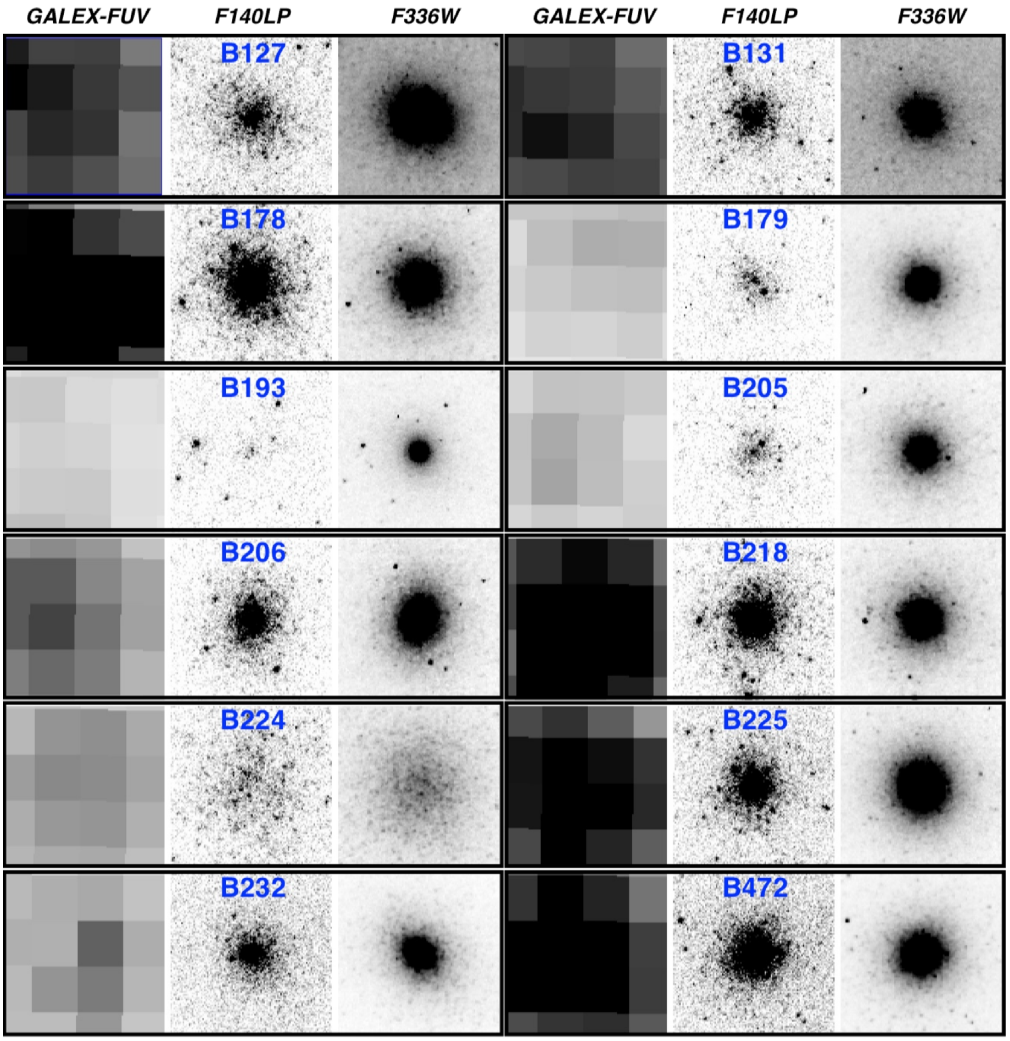

Figure 1. Thumbnails of the 12 globular clusters studied. From top left to bottom right, these are B127, B131, B178, B179, B193, B205, B206, B218, B224, B225, B232, B472, respectively. For each cluster, we show observations from *GALEX* FUV, *HST* ACS/SBC F140LP, and *HST* WFC3/UVIS F336W, left to right, respectively. Each image is 5 arcsec × 5 arcsec.

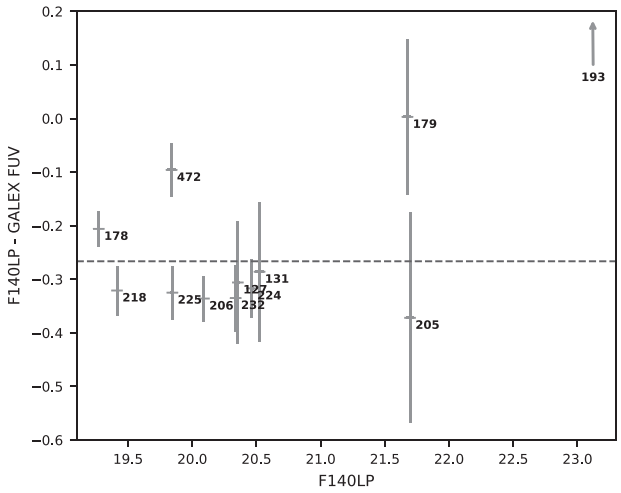

Figure 2. A comparison of the FUV magnitudes of M 31's globular clusters from published *GALEX* FUV photometry and our *HST* ACS/SBC *F140LP* photometry.

Vanderbeke et al. (2015) drew similar conclusions to our surface brightness profiles of M 31's globular clusters, with 80 per cent of their Galactic globular cluster sample having similarly distributed HB stars. Some of the remaining clusters did show centrally concentrated extreme HB populations, while they were less concentrated in three of the clusters.

Below we discuss possible implications and origins of the well mixed FUV bright populations observed in M 31's clusters.

4 DYNAMICAL FORMATION OF EXTREME-HB STARS

Dynamical interactions between stars in the dense cores of globular clusters may enhance the formation of extreme-HB stars. Several processes have been proposed to produce new or hotter HB stars in such dense environments, including helium dredge up in close interactions; enhanced mass-loss in tightened binary systems; and the merger of two white dwarfs to produce an extreme-HB-like star (as discussed in Section 1).

Some observations of the Galactic globular clusters suggest that dynamical interactions may produce bluer HB stars, with measures

Downloaded from https://academic.oup.com/mnras/article-abstract/481/3/3313/5094594 by University of Southampton user on 07 November 2018

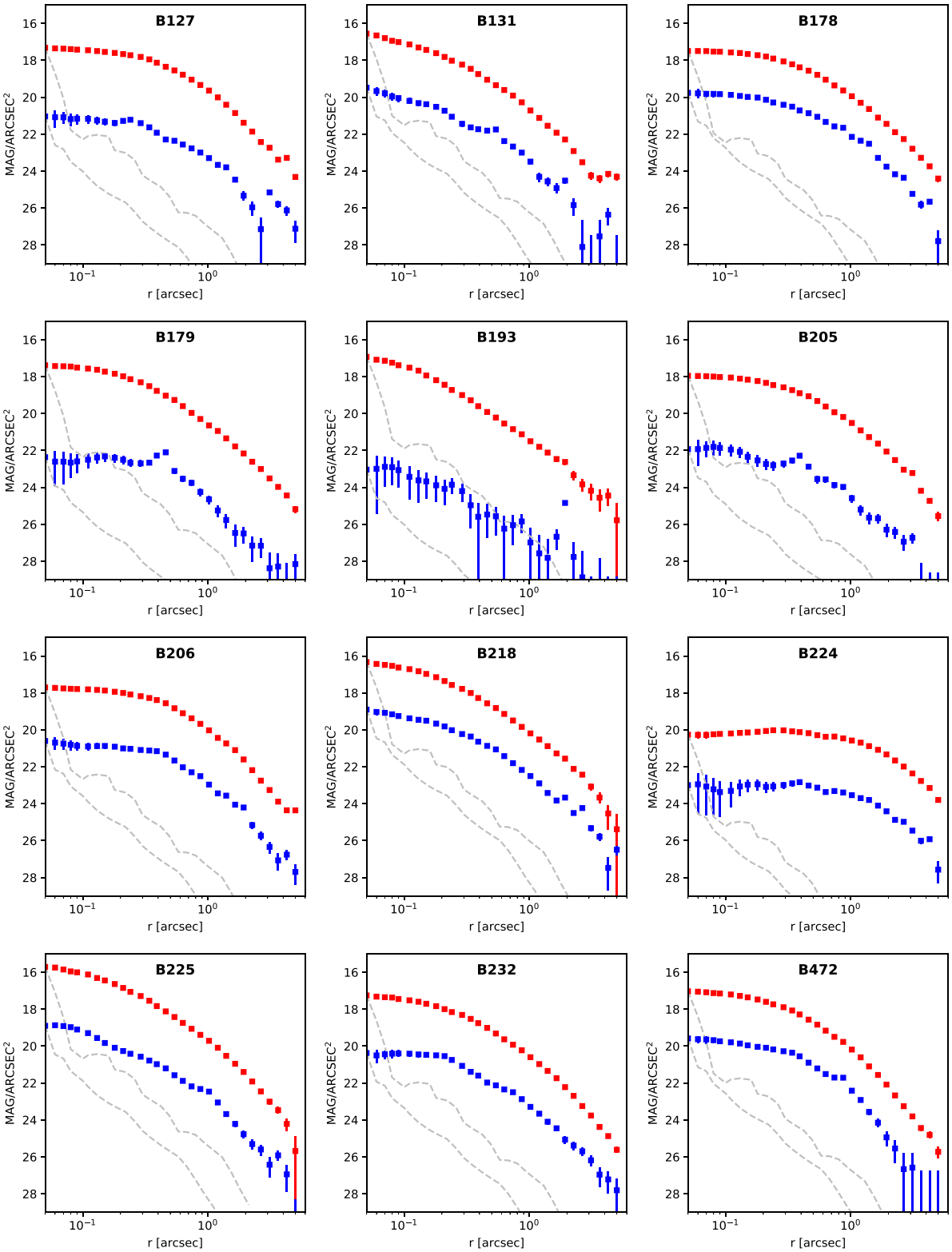

Figure 3. Surface brightness profiles (mag arcsec^2) of the 12 globular clusters through the F140LP (blue points) and F336W (red points) filters. Grey-dashed lines show the expected profiles of a point source, based on the TinyTim simulator and scaled to have the same surface brightness as the clusters at 0.05 arcsec.

of the clusters' HB temperatures correlating with the stellar density (e.g. Fusi Pecci et al. 1993; Buonanno et al. 1997; Rich et al. 1997; Dotter et al. 2010). However, other studies have proposed a lack of correlation (e.g. van den Bergh & Morris 1993; Recio-Blanco et al. 2006; Dalessandro et al. 2012). In M 31's clusters, it has previously been shown that their $FUV - NUV$ colour correlates with stellar density, with denser clusters having bluer $FUV - NUV$ (Peacock et al. 2011). In Fig. 5, we show that this trend is reproduced by

Downloaded from https://academic.oup.com/mnras/article-abstract/481/3/3313/5094594 by University of Southampton user on 07 November 2018

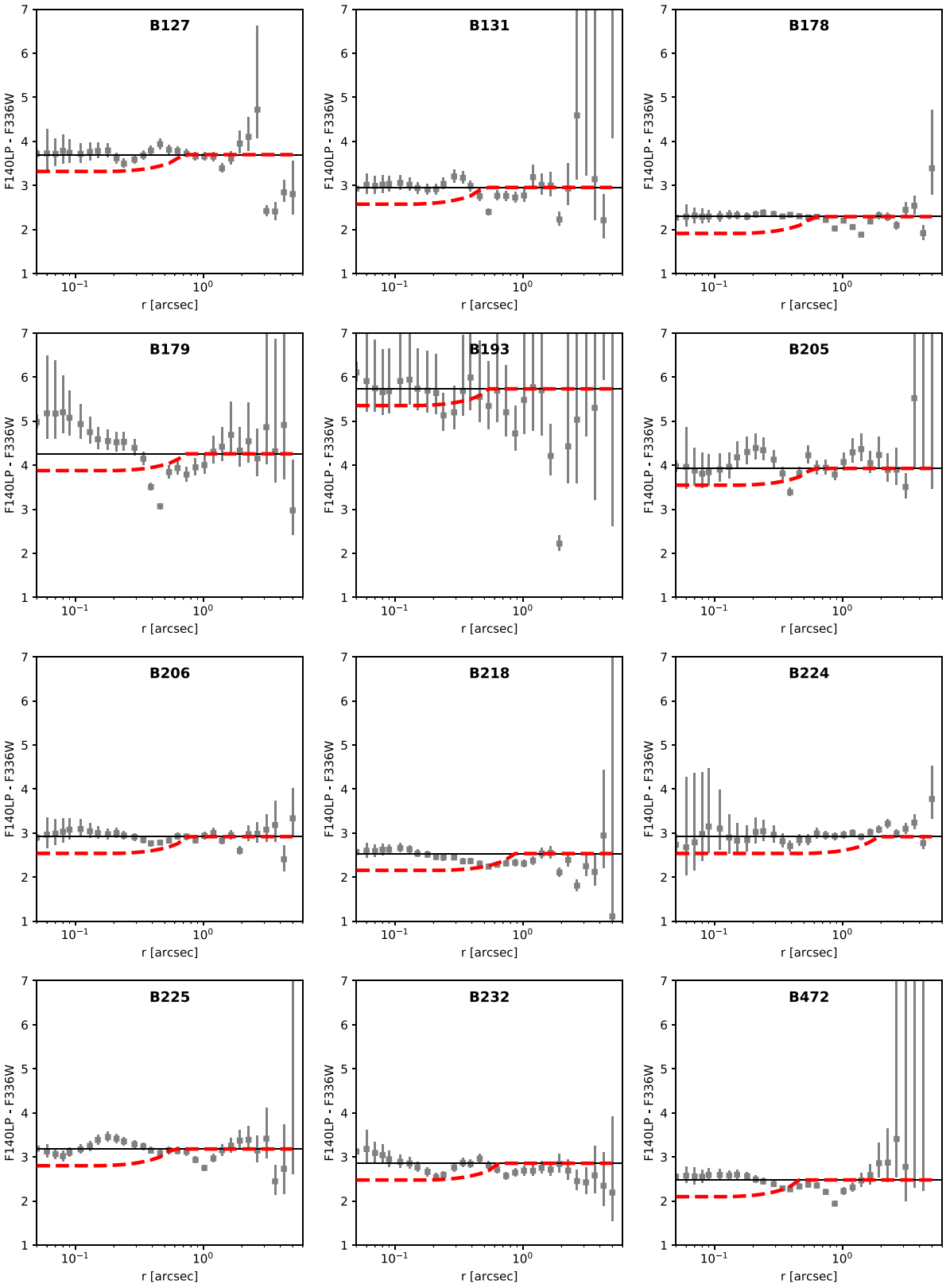

Figure 4. $F140LP - F336W$ ($FUV - u$) profiles of 12 of M 31's old globular clusters. The solid black line shows the weighted mean colour out to 5 arcsec. The red-dashed line shows the predicted profiles if the clusters host centrally concentrated second populations of helium-enhanced stars, similar to those observed in the Galactic globular clusters by Lardo et al. (2011, see Section 5.2).

Downloaded from https://academic.oup.com/mnras/article-abstract/481/3/3313/5094594 by University of Southampton user on 07 November 2018

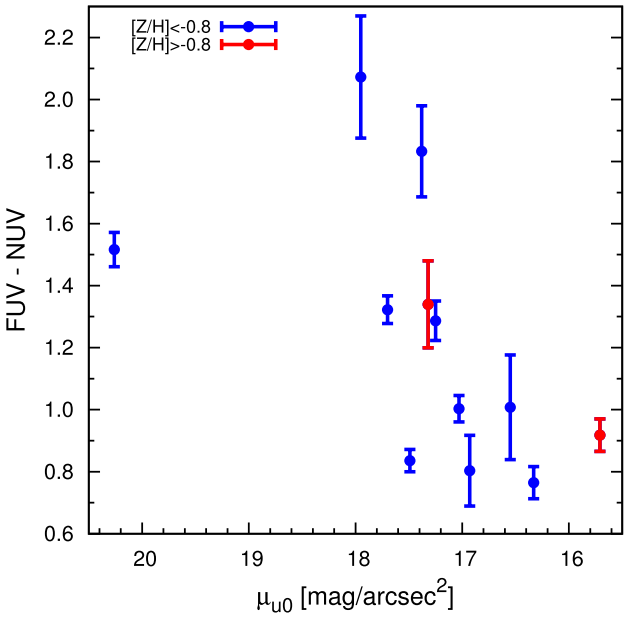

Figure 5. The integrated *GALEX FUV* − *NUV* colour of our sample of M 31's clusters as a function of central stellar density. Metal-rich ([*Z*/*H*] > −0.8) and metal-poor clusters are identified as red and blue points, respectively. We note that B193 is excluded from this plot, since we believe its *GALEX* colours may be unreliable (see Section 3.2).

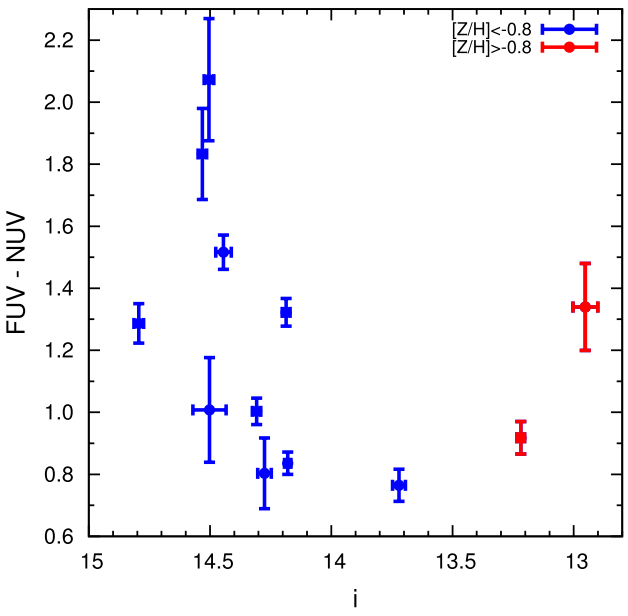

Figure 6. Same as Fig. 5, but comparing *FUV* − *NUV* to total *i*-band magnitude.

our sample of clusters with *FUV* − *NUV* correlating with central *u*-band surface brightness. We also show *FUV* − *NUV* as a function of the total *i*-band magnitude of the clusters (Fig. 6). This shows a similar trend, which is unsurprising, given that cluster mass is known to correlate with central stellar density (e.g. McLaughlin & van der Marel 2005; Peacock et al. 2010b). One explanation for this correlation is that denser and more massive clusters are brighter in the FUV due to increased dynamical interactions producing bluer HB stars and hence more FUV emission.

A key signature of a dynamically enhanced population is it should be centrally concentrated – since it will be preferentially produced in the cluster cores, where the stellar density is highest. This is observed for another population of dynamically enhanced systems, low-mass X-ray binaries. These systems are generally found in the core regions of Galactic globular clusters and do preferentially reside in denser clusters with higher interaction rates (Bellazzini et al. 1995; Pooley et al. 2003; Peacock et al. 2009). It is also worth noting that the lifetimes of HB stars are typically an order of magnitude less than the half-light relaxation times of these clusters. It is therefore unlikely centrally formed extreme-HB stars have become significantly mixed with the other populations.

None of the clusters in our sample are observed to have significantly bluer cores (see Fig. 4). We therefore conclude that there is no evidence that the excess FUV emission from these dense clusters is the result of dynamical interactions producing significant populations of extreme-HB stars. We note that this is despite our sample including clusters with very high central densities and hence high stellar interaction rates (see Table 1). Indeed, the presence of LMXBs in two of these clusters confirms that stellar interactions are occurring (B193 and B225; Trudolyubov & Priedhorsky 2004; Peacock et al. 2010b). An alternate explanation for these FUV bright clusters is therefore preferred, such as subpopulations of helium-enriched stars (discussed in Section 5 below).

5 SECOND POPULATIONS IN M 31'S GLOBULAR CLUSTERS

It is now well established that the Galactic globular clusters host multiple stellar populations. While a comprehensive model for the formation of multiple populations in globular clusters is still lacking, most theories require hydrogen burning at high temperatures in order to reproduce the observed light element abundance variations. Therefore, second population stars are expected to be helium enhanced.

These different helium abundances can produce the observed split/broadened main sequences and red giant branches. However, their most dramatic effect is on the HB star morphology, since helium-enhanced populations are expected to produce HB stars with much higher surface temperatures. It has been shown that the HB star morphologies of some Galactic globular clusters can be explained by including helium-enhanced populations (e.g. D'Antona et al. 2005; Joo & Lee 2013; Lee et al. 2005). Further evidence comes from a correlation between size of the spread in the light element abundance of second population stars in a cluster with the maximum temperature of its HB stars (Carretta et al. 2010a), while Marino et al. (2011) observed the Na and O abundances of red- and blue-HB stars in M4 and found that they were consistent with those of the first and second generations, respectively.

The bluer HB stars produced by helium-enriched second populations provide a signature for detecting second populations in extra-galactic globular clusters. This is because a population of blue-/extreme-HB stars will dominate the integrated FUV emission from a cluster. Interestingly, Peacock et al. (2017) showed that extragalactic globular clusters in M 31 (Rey et al. 2007), M81 (Mayya et al. 2013), and M87 (Sohn et al. 2006; Peacock et al. 2017) often have bluer *FUV* − *V* colours than expected for simple stellar populations models with standard helium abundances.

In Fig. 7, we plot the FUV and optical colours of the M 31 clusters studied here along with published FUV and optical colours of other clusters. Specifically, we include published FUV colours of clusters in the Milky Way (Sohn et al. 2006; Dalessandro et al. 2012), M87

Downloaded from https://academic.oup.com/mnras/article-abstract/481/3/3313/5094594 by University of Southampton user on 07 November 2018

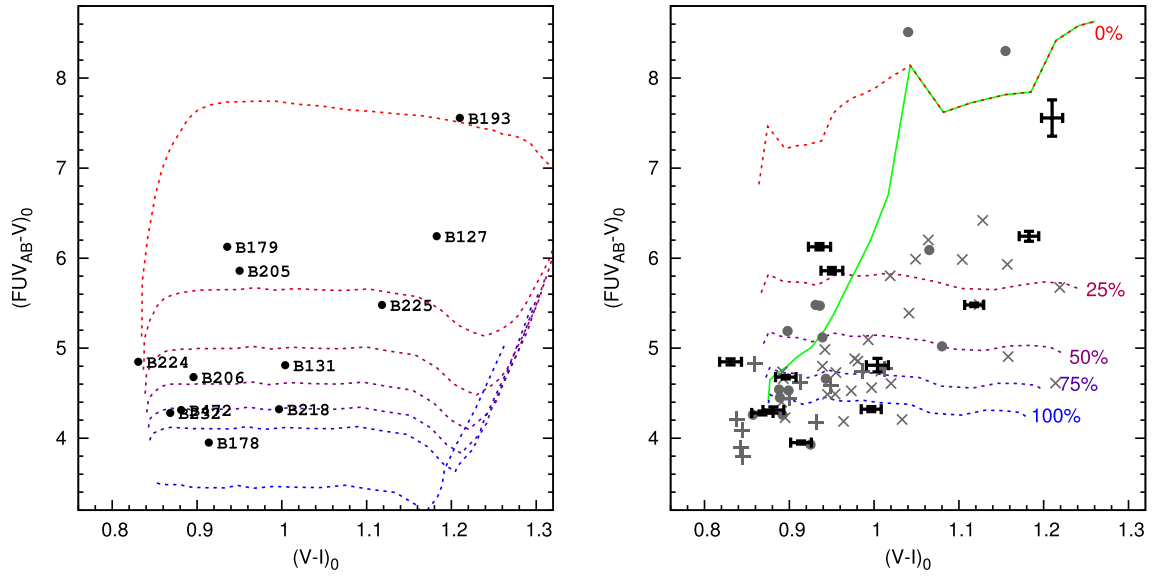

Figure 7. Integrated $FUV - V$ of M 31's clusters as a function of their $V - I$ optical colour (labelled points in the left-hand panel and black points with errorbars in the right-hand panel). In the right-hand panel, we also show clusters in the Milky Way (grey points), other clusters in M 31 (grey pluses) and M87 (grey crosses). Only quite massive clusters (those with $M_V < -9.0$) are included, this reduces stochastic effects in the $FUV - V$ colour. The left-hand panel shows predicted colours from the YPES models of Chung, Yoon & Lee (2017). These are for a stellar population that is composed of a primordial population with helium fraction, $Y = 0.23$, and a second helium-enhanced population with $Y = 0.38$ (where the fraction of second population stars is 0, 10, 20, 30, 40, 50, 100 per cent, red to blue lines). The right-hand panel compares these data to the FSPS models of Conroy, Gunn & White (2009), where the fractions of blue- to red-HB stars is 0, 25, 50, 75, 100 per cent, red to blue lines. The green lines shows the variation predicted due to the influence of metallicity on the HB star population.

(Sohn et al. 2006; Peacock et al. 2017) and other clusters in M 31 (from *GALEX* observations; Rey et al. 2007). We limit this sample to only include quite massive clusters, those with $M_V < -9.0$. This ensures that the clusters have relatively large populations that reduces stochastic effects in the FUV colours. For details of these extragalactic cluster data, see Peacock et al. (2017, and references therein).

To interpret these cluster colours, we compare to predictions based on two different stellar populations synthesis models. We note that there is significant uncertainty in modelling the properties of the HB stars in a stellar population and these models are intended as a guide to the effect of including second populations of helium-enhanced stars, rather than a precise comparison. The left-hand panel shows the YPES models of Chung et al. (2017) for an 11 Gyr population with metallicity in the range $-2.6 < [Z/H] < 0.6$ for clusters hosting two populations of stars; one with primordial helium abundances ($Y = 0.23$) and the other with enhanced helium abundances ($Y = 0.38$). The fraction of the helium-enhanced second population is 0, 10, 20, 30, 40, 50, 100 per cent (red to blue lines, respectively). The right-hand panel shows models from the FSPS models (Conroy et al. 2009; Conroy & Gunn 2010). These are based on the PADOVA stellar isochrones and BASEL stellar libraries for a 12 Gyr simple stellar population with metallicity in the range $-2.0 < [Z/H] < 0.0$. We plot models with different fractions of blue- to red-HB stars: 0, 25, 50, 75, 100 per cent, red to blue lines, respectively. The green solid line in Fig. 7 shows the predicted variation due to metallicity, where the population varies from having only blue-HB stars at low metallicity to only red-HB stars at high metallicity.

The predicted cluster colours vary due to both the different models used and the details of the populations assumed. However, the general trend is very similar and consistent with the empirical conclusions based on the Milky Way's clusters; that increasing the fraction of helium-enhanced second population stars produces bluer HB stars and hence bluer $FUV - V$ colours (see also the models considered in Rey et al. 2007 for similar conclusions).

Metallicity is known to influence the HB population of clusters, with metal-rich globular clusters producing red-HB stars for standard helium abundances. These relatively cool HB stars should result in very red $FUV - V$ colours, such as the Galactic globular cluster 47 Tuc and the cluster B193 from this study. However, two of the metal rich clusters in our sample (B127 and B225) have bluer colours than predicted based on their metallicity, suggesting the presence of a significant fraction of helium-enhanced second population stars. These clusters may be analogous to the metal-rich Galactic globular cluster NGC 6441, which has both red-HB stars and a tail of much hotter HB stars resulting in its relatively bright FUV emission. We note that similarly *FUV* bright metal-rich clusters are also observed in the Milky Way (NGC 6388 and NGC 6441), M87 (Sohn et al. 2006; Peacock et al. 2017), and M81 (GC1; Mayya et al. 2013).

Metal-poor globular clusters tend to host blue HB populations for standard helium abundances. This means that the presence of second populations of hotter helium-enhanced stars has less of an influence on their integrated $FUV - V$ colour. However, significant variation is observed at a given $V - I$ (or metallicity) with the clusters B131, B178, and B218 having relatively blue $FUV - V$ for their metallicity – these could be explained by the presence of higher fractions (or more helium-enhanced) second populations with hotter HB stars. The integrated colours of some of the clusters in our sample are therefore consistent with the presence of second

Downloaded from https://academic.oup.com/mnras/article-abstract/481/3/3313/5094594 by University of Southampton user on 07 November 2018

populations of helium-enhanced stars, similar to those observed in the Milky Way.

Perina et al. (2012) have previously studied the HB populations of M 31's outer halo globular clusters based on optical *HST* colour–magnitude diagrams. Interestingly, they observed that their sample of clusters have slightly redder HB morphology for a given metallicity than the Galactic clusters. A possible explanation is that these clusters are slightly younger than the Galactic comparison sample, potentially consistent with their location in the outer halo and substructure association. Such work represents a complimentary approach to integrated FUV observations. The resolved CMDs allow direct counts of stars redder and bluer than the instability strip, but are less sensitive to the hottest HB stars. Similar to our conclusions, Perina et al. (2012) showed that integrated FUV emission from some of their sample are consistent with extreme-HB stars and that the ratio of red to blue-HB stars in some metal rich clusters (G1 and B045) may suggest the presence of multiple populations.

5.1 A correlation between the mass/density of M 31's clusters and their second populations?

As discussed in Section 4, M 31's clusters show a trend such that more massive, denser clusters are bluer in $FUV - NUV$ (see Figs 5 and 6). The $FUV - NUV$ colour is sensitive to the temperature of the HB star populations. Second populations in these clusters could explain this trend, if their fraction or helium abundance correlates with cluster mass (and hence density). This would produce hotter HB stars in denser clusters and hence the bluer ultraviolet colour. Interestingly, such a trend has been proposed in the Milky Way's globular clusters, where the helium enhancement of the second population appears to correlate with cluster mass (e.g. Carretta et al. 2010a; Milone et al. 2017). The trends observed in Figs 5 and 6 can therefore be interpreted as evidence that M 31's clusters host similar second populations of stars to the Milky Way, with their helium enhancement (and hence HB star temperatures) correlating with the mass and density of the clusters. This is also consistent with spectroscopic observations of M31's clusters which show a correlation between the abundance of second population sensitive light elements (N and Na) and cluster mass (Schiavon et al. 2013; Sakari et al. 2016).

5.2 Spatially distinct second populations

Some theories for the formation of multiple populations produce the second population centrally within the clusters. This is advantageous because, as the cluster evolves, it preferentially loses stars from the less concentrated first population – hence reducing the mass budget problem. Simulations have shown that, if the relaxation times of the clusters are long enough, these populations can remain spatially distinct for a Hubble time (e.g. Vesperini et al. 2013). Therefore, identifying whether multiple populations are spatially distinct can place important constraints for theories of their formation.

Several independent studies have observed centrally concentrated second populations in the Galactic globular clusters. Lardo et al. (2011) used SDSS observations of red giant branch stars to identify centrally concentrated second populations in seven out of the nine clusters they studied (over the radial range $0.5r_h < r < 5r_h$). Observations of individual clusters have drawn similar conclusions (e.g. Carretta et al. 2010b; Kravtsov et al. 2011; Beccari et al. 2013; Simioni et al. 2016). However, there are some exceptions with evidence for well mixed populations in some clusters (Dalessandro et al. 2014; Vanderbeke et al. 2015) and even less concentrated second populations (Lim et al. 2016; Dalessandro et al. 2018). Additionally, studies utilizing the HB star temperature as a tracer of first and second population stars found the populations to be well mixed in many clusters (Iannicola et al. 2009; Vanderbeke et al. 2015). If present, the lack of radial signatures identified in some of the Galactic clusters may be due to observing different radial regions (and associated relaxation times) or the sensitivity of different techniques for identifying the populations. Additionally, we note that cluster-to-cluster variations are expected due to differing relaxation times and known differences in both the fractions and abundances of their second populations.

5.2.1 *Testing for spatially distinct populations in M 31s clusters*

The FUV profiles of M 31's clusters – particularly those whose FUV colours suggest the presence of multiple populations – can potentially extend this work to clusters beyond the Milky Way. If the second population is centrally concentrated, one would expect 'excess' FUV emission from the bluer second population HB stars to be more concentrated than the emission at redder wavelengths (which will probe the combined population).

Modelling the potential effects on the integrated $FUV - u$ profiles is challenging, since it involves both a model for the radial distribution of the first and second populations and how these influence the ultraviolet colours. To give an idea of the potential profiles that may be expected, we assume that the clusters have multiple populations with a similar distribution to those observed in the Galactic globular clusters by Lardo et al. (2011). Specifically, we assume the number of stars in the second population are similar to those in the first population for $r > 3r_h$ and increase linearly to become three times bigger for $r < 1r_h$. The resulting change in $FUV - u$ is estimated using the YPES models, where the two populations are assumed to have helium fractions, $Y = 0.23$ and 0.33.

The red line in Fig. 4 shows this predicted variation in the colour profile. It can be seen that such gradients may be detectable in data with this resolution. However, none of the clusters show the signature of significantly bluer $FUV - u$ colours towards their cores. Surprisingly, B218 is observed to actually have slightly redder colours in its central regions.

We caution that there is significant uncertainty in the plotted prediction and that the profile shown is intended as an example of the possible variation, rather than a comprehensive model. First, the expected fraction and distribution of the populations is not very well constrained by the Galactic clusters and is likely to vary from cluster to cluster. Additionally, the resulting colour change is dependent on both the details of the population abundances and the stellar populations models. We therefore note the lack of any evidence for strong radial variations over the range observed by Lardo et al. (2011) in the Galactic globular clusters, but are unable to rule out radially distinct multiple populations. However, we do note that such data are sensitive to radial variations in the HB populations over radial ranges observed in some Galactic globular clusters.

6 SUMMARY

We present the ultraviolet surface brightness density profiles of 12 massive globular clusters in M 31 based on high-resolution *HST* photometry. We find no evidence for differences in the surface brightness profiles of the clusters in F140LP-F336W ($FUV - u$). We note that this colour is very sensitive to the temperatures of HB

Downloaded from https://academic.oup.com/mnras/article-abstract/481/3/3313/5094594 by University of Southampton user on 07 November 2018

stars in these clusters and that the similar profiles observed suggest no evidence for a population of spatially distinct blue-/extreme-HB stars.

Our FUV photometry shows that some of these clusters are brighter in the *FUV* than expected based on canonical models. This is consistent with similar conclusions based on *GALEX* and *HST* observations of other clusters. We consider two scenarios for the production of this extra FUV emission; dynamical interactions enhancing the population of extreme-HB stars and the presence of second populations of helium-enhanced HB stars that are hotter than their primordial counterparts.

Dynamically enhanced populations should be formed in the cluster cores, where the stellar density is highest. Given that HB stars have quite short lifetimes, we expect such a population to still be centrally located. The lack of centrally concentrated FUV emission in these clusters therefore argues against a dynamically enhanced extreme-HB population as the origin of the enhanced FUV emission.

The excess FUV emission observed from these clusters is consistent with the clusters hosting second populations of helium-enhanced stars. Additionally, we note that the correlation between $FUV - NUV$ and the stellar density/mass of clusters suggests that the fraction (or helium enhancement) of these second-generation stars correlates with these parameters. Such correlations have been observed in the Galactic globular clusters. Our results are therefore consistent with M 31's clusters hosting similar second populations of stars to the Galactic globular clusters. We note that there is no evidence that this second population is centrally concentrated within the clusters.

ACKNOWLEDGEMENTS

MBP, AK, and TJM acknowledge support from *HST*-GO-14132. MBP and SEZ acknowledge support from the NSF grant AST-1412774. JS acknowledges support from NSF grant AST-1514763 and a Packard Fellowship.

Based on observations made with the NASA/*ESA*, obtained from the data archive at the Space Telescope Science Institute. STScI is operated by the Association of Universities for Research in Astronomy, Inc., under NASA contract NAS 5-26555. Support for this work was provided by NASA through grant number *HST*-GO-14132.001-A from the Space Telescope Science Institute, which is operated by AURA, Inc., under NASA contract NAS 5-26555.

REFERENCES

Barmby P., McLaughlin D. E., Harris W. E., Harris G. L. H., Forbes D. A., 2007, AJ, 133, 2764
Bastian N., 2015, preprint (arXiv:1510.01330)
Bastian N., Lardo C., 2018, Annual Review of Astronomy and Astrophysics, 56, 83
Beccari G., Bellazzini M., Lardo C., Bragaglia A., Carretta E., Dalessandro E., Mucciarelli A., Pancino E., 2013, MNRAS, 431, 1995
Bellazzini M., Pasquali A., Federici L., Ferraro F. R., Pecci F. F., 1995, ApJ, 439, 687
Bellazzini M., Pecci F. F., Ferraro F. R., Galleti S., Catelan M., Landsman W. B., 2001, AJ, 122, 2569
Binney J., Tremaine S., 1987, Galactic Dynamics, Princeton University Press, Princeton, NJ
Boffi F., Sirianni M., Lucas R., Walborn N., Proffitt C., 2008, Technical Instrument Report ACS, 2008-002. STScI, Baltimore, MD, USA
Bragaglia A. et al., 2010, ApJ, 720, L41
Brown T. M., Bowers C. W., Kimble R. A., Sweigart A. V., Ferguson H. C., 2000, ApJ, 532, 308
Brown T. M., Ferguson H. C., Smith E., Kimble R. A., Sweigart A. V., Renzini A., Rich R. M., VandenBerg D. A., 2004, ApJ, 613, L125
Brown T. M., Smith E., Ferguson H. C., Sweigart A. V., Kimble R. A., Bowers C. W., 2008, ApJ, 682, 319
Buonanno R., Corsi C., Bellazzini M., Ferraro F. R., Pecci F. F., 1997, AJ, 113, 706
Cardelli J. A., Clayton G. C., Mathis J. S., 1989, ApJ, 345, 245
Carretta E., Bragaglia A., D'Orazi V., Lucatello S., Gratton R. G., 2010b, A&A, 519, A71
Carretta E., Bragaglia A., Gratton R. G., Recio-Blanco A., Lucatello S., D'Orazi V., Cassisi S., 2010a, A&A, 516, A55
Catelan M., 2009, Ap&SS, 320, 261
Chung C., Yoon S.-J., Lee Y.-W., 2011, ApJ, 740, L45
Chung C., Yoon S.-J., Lee Y.-W., 2017, ApJ, 842, 91
Code A. D., 1969, PASP, 81, 475
Colucci J. E., Bernstein R. A., Cameron S., McWilliam A., Cohen J. G., 2009, ApJ, 704, 385
Conroy C., Gunn J. E., 2010, ApJ, 712, 833
Conroy C., Gunn J. E., White M., 2009, ApJ, 699, 486
Dalcanton J. J. et al., 2012, ApJS, 200, 18
Dalessandro E., Schiavon R. P., Rood R. T., Ferraro F. R., Sohn S. T., Lanzoni B., O'Connell R. W., 2012, AJ, 144, 126
Dalessandro E. et al., 2014, ApJ, 791, L4
Dalessandro E. et al., 2018, ApJ, 859, 15
Dorman B., O'Connell R. W., Rood R. T., 1995, ApJ, 442, 105
Dotter A. et al., 2010, ApJ, 708, 698
D'Antona F., Bellazzini M., Caloi V., Pecci F. F., Galleti S., Rood R. T., 2005, ApJ, 631, 868
D'Antona F., Ventura P., 2007, MNRAS, 379, 1431
Fan Z., Ma J., de Grijs R., Zhou X., 2008, MNRAS, 385, 1973
Fusi Pecci F., Ferraro F. R., Bellazzini M., Djorgovski S., Piotto G., Buonanno R., 1993, AJ, 105, 1145
Gratton R. G., Carretta E., Bragaglia A., 2012, A&A Rev., 20, 50
Greggio L., Renzini A., 1990, ApJ, 364, 35
Han Z., 2008, A&A, 484, L31
Han Z., Podsiadlowski P., Lynas-Gray A. E., 2007, MNRAS, 380, 1098
Han Z., Podsiadlowski P., Maxted P. F. L., Marsh T. R., 2003, MNRAS, 341, 669
Heggie D. C., 1975, MNRAS, 173, 729
Iannicola G. et al., 2009, ApJ, 696, L120
Joo S.-J., Lee Y.-W., 2013, ApJ, 762, 36
Kravtsov V., Alcaíno G., Marconi G., Alvarado F., 2011, A&A, 527, L9
Krist J. E., Hook R. N., Stoehr F., 2011, Optical Modeling and Performance Predictions V
Lardo C., Bellazzini M., Pancino E., Carretta E., Bragaglia A., Dalessandro E., 2011, A&A, 525, A114
Larsen S. S., 1999, A&AS, 139, 393
Lee Y. et al., 2005, ApJ, 621, L57
Lim D., Lee Y.-W., Pasquato M., Han S.-I., Roh D.-G., 2016, ApJ, 832, 99
Maraston C., 2005, MNRAS, 362, 799
Marino A. F., Villanova S., Milone A. P., Piotto G., Lind K., Geisler D., Stetson P. B., 2011, ApJ, 730, L16
Marino A. F. et al., 2014, MNRAS, 437, 1609
Maxted P. f. L., Heber U., Marsh T. R., North R. C., 2001, MNRAS, 326, 1391
Mayya Y. D., Rosa-González D., Santiago-Cortés M., Rodríguez-Merino L. H., Vega O., Torres-Papaqui J. P., Bressan A., Carrasco L., 2013, MNRAS, 436, 2763
McLaughlin D. E., van der Marel R. P., 2005, ApJS, 161, 304
Milone A. P., 2015, MNRAS, 446, 1672
Milone A. P. et al., 2012, ApJ, 744, 58
Milone A. P. et al., 2017, MNRAS, 464, 3636
Moehler S., 2001, PASP, 113, 1162
O'Connell R. W., 1999, ARA&A, 37, 603

Downloaded from https://academic.oup.com/mnras/article-abstract/481/3/3313/5094594 by University of Southampton user on 07 November 2018

Pasquato M., de Luca A., Raimondo G., Carini R., Moraghan A., Chung C., Brocato E., Lee Y.-W., 2014, ApJ, 789, 28
Pasquini L., Mauas P., Käufl H. U., Cacciari C., 2011, A&A, 531, A35
Peacock M. B., Maccarone T. J., Knigge C., Kundu A., Waters C. Z., Zepf S. E., Zurek D. R., 2010a, MNRAS, 402, 803
Peacock M. B., Maccarone T. J., Kundu A., Zepf S. E., 2010b, MNRAS, 407, 2611
Peacock M. B., Maccarone T. J., Waters C. Z., Kundu A., Zepf S. E., Knigge C., Zurek D. R., 2009, MNRAS, 392, L55
Peacock M. B., Zepf S. E., Kundu A., Chael J., 2017, MNRAS, 464, 713
Peacock M. B., Zepf S. E., Maccarone T. J., Kundu A., 2011, ApJ, 737, 5
Perina S., Bellazzini M., Buzzoni A., Cacciari C., Federici L., Fusi Pecci F., Galleti S., 2012, A&A, 546, A31
Piotto G., Milone A. P., Marino A. F., Bedin L. R., Anderson J., Jerjen H., Bellini A., Cassisi S., 2013, ApJ, 775, 15
Pooley D. et al., 2003, ApJ, 591, L131
Recio-Blanco A., Aparicio A., Piotto G., de Angeli F., Djorgovski S. G., 2006, A&A, 452, 875
Rey S.-C. et al., 2007, ApJS, 173, 643
Rey S. et al., 2009, ApJ, 700, L11
Rich R. M. et al., 1997, ApJ, 484, L25
Sakari C. M. et al., 2016, ApJ, 829, 116
Sandage A., Wallerstein G., 1960, ApJ, 131, 598
Schiavon R. P. et al., 2013, ApJ, 776, 7
Simioni M., Milone A. P., Bedin L. R., Aparicio A., Piotto G., Vesperini E., Hong J., 2016, MNRAS, 463, 449
Smith R. J., Lucey J. R., Carter D., 2012, MNRAS, 421, 2982
Sohn S. T., O'Connell R. W., Kundu A., Landsman W. B., Burstein D., Bohlin R. C., Frogel J. A., Rose J. A., 2006, AJ, 131, 866
Strader J., Caldwell N., Seth A. C., 2011, AJ, 142, 8
Suda T., Tsujimoto T., Shigeyama T., Fujimoto M. Y., 2007, ApJ, 671, L129
Trudolyubov S., Priedhorsky W., 2004, ApJ, 616, 821
van den Bergh S., Morris S., 1993, AJ, 106, 1853
Vanderbeke J., De Propris R., De Rijcke S., Baes M., West M., Alonso-García J., Kunder A., 2015, MNRAS, 451, 275
Vesperini E., McMillan S. L. W., D'Antona F., D'Ercole A., 2013, MNRAS, 429, 1913
Vilardell F., Ribas I., Jordi C., Fitzpatrick E. L., Guinan E. F., 2010, A&A, 509, A70
Wagner-Kaiser R., Stenning D. C., Sarajedini A., von Hippel T., van Dyk D. A., Robinson E., Stein N., Jefferys W. H., 2016, MNRAS, 463, 3768
Williams B. F. et al., 2014, ApJS, 215, 9
Yaron O., Prialnik D., Kovetz A., Shara M. M., 2017, preprint (arXiv: 1709.02127)
Yi S. K., Lee J., Sheen Y.-K., Jeong H., Suh H., Oh K., 2011, ApJS, 195, 22

This paper has been typeset from a TEX/LATEX file prepared by the author.

Downloaded from https://academic.oup.com/mnras/article-abstract/481/3/3313/5094594 by University of Southampton user on 07 November 2018